The characteristics of evapotranspiration and crop coefficients of an irrigated vineyard in arid Northwest China

Shangtao Wang, Gaofeng Zhu[*], Dunsheng Xia, Jinzhu Ma, Tuo Han, Ting Ma, Kun Zhang, Shasha Shang

Key Laboratory of Western China's Environmental Systems (Ministry of Education), College of Earth and Environmental Sciences, Lanzhou University, 222 South Tianshui Road, Lanzhou, 730000, China

ARTICLE INFO

ABSTRACT

Oasis effect may have significant impacts on the crop water use in irrigated fields of extremely arid conditions. Studies on crop coefficients and its relevant influence factors are essential to accurately determine the irrigation scheduling under such conditions. A two-year experiment was conducted in an irrigated vineyard to estimate evapotranspiration (ET) and its two components: evaporation (E) and crop transpiration (T), and to develop appropriate region-specific crop coefficients (K_c, K_{cb}) in arid Northwest China. The contributions of "oasis effect" to K_c, the relationships of both K_c and K_{cb} to canopy conductance (G_c) and leaf area index (LAI) were investigated. Local values of K_c for evapotranspiration and crop transpiration (K_{cb}) were calculated using the field data and the dual-K_c approach. The daily ET ranged from 0.80 to 9.87 mm d^{-1} and from 0.99 to 8.73 mm d^{-1} in 2014 and 2015, respectively, with corresponding T/ET values amounting to approximately 58.4% and 55.1%. The locally averaged K_c values were 0.79, 1.31, and 1.08 during the initial, middle, and late growth stages, respectively, versus corresponding K_{cb} values of 0.17, 0.97, and 0.64. Arid advection accounted for 16.9 to 57.4% and from 1.4 to 49.0% of daily K_c during the two study periods. Both K_c and K_{cb} to LAI is a linear regression but to G_c is an exponential one. LAI is a better indicator than G_c when it is used to predict K_c and K_{cb}. These results will help growers to improve irrigation efficiency and quantify the contributions of individual factors to K_c and K_{cb} in such conditions.

1. Introduction

Evapotranspiration (ET) is a significant process in terrestrial systems, where it represents a link among the hydrological, carbon, and energy cycles (Zhu et al., 2016a, b). About 60% of rainfall re-enters the atmosphere through transpiration (T) and evaporation (E), but this amount can reach 90% in agricultural ecosystems (Jung et al., 2010; Zhu et al., 2014). Thus, accurate measurement and estimation of ET and its components (T and E) in agricultural ecosystems are crucial both for managing irrigation and for improving crop yield (Allen et al., 2011; Sun et al., 2012; Kool et al., 2014; Zhao and Zhao, 2015). Many techniques have been developed to measure ET and its components, such as combining the sap-flow and eddy-covariance methods (Herbst et al., 1996; Cavanaugh et al., 2011; Zhang et al., 2011), developing land-surface models (Oleson et al., 2004; Dirmeyer et al., 2006), and isotope methods (Williams et al., 2004; Wang et al., 2010; Jasechko et al., 2013). Of these methods, the combination of sap-flow and eddy-covariance techniques supply a direct and robust observation of ET and T,

and therefore provide basic data that can be used to assess the accuracy of other methods. Thus, this combination has been widely used to measure and partition the components of ET in various ecosystems (Ding et al., 2015).

In comparison with direct in situ measurements, accurately estimating ET based on meteorological data is appealing in irrigation scheduling due to its relative simplicity and ease of application (Jagtap and Jones, 1989; Ding et al., 2015). The dual crop coefficient (dual-K_c) method proposed by the Food and Agriculture Organization (FAO-56) has been widely used to estimate the components of ET (Allen et al., 1998). In this method, the crop coefficient (K_c) is partitioned into two parts: the basal crop coefficient (K_{cb}), representing crop transpiration and the soil evaporation coefficient (K_e). This method has been extensively applied in different crop ecosystems, including coffee (Flumignan et al., 2009), castor (Campbell et al., 2015), apple trees (Marsal et al., 2013), peach orchard (Paço et al., 2012), and grapevines (Fandiño et al., 2012; Picón-Toro et al., 2012; Poblete-Echeverría and Ortega-Farias, 2013; Zhao et al., 2015). However, the values of the crop

coefficients (K_c or K_{cb}) have been reported to be sensitive to climate, hydrological, and environmental factors. As a result, the proposed adjustment method for K_c and K_{cb} in FAO-56 can only approximately explain the variations of K_c and K_{cb} in response to changes in relative humidity (*RH*), wind speed, and other environmental variables (Allen et al., 1998). Significant uncertainties in estimating *ET* and its components have been reported in previous studies when directly using the FAO-proposed coefficient values in different regions (Sánchez et al., 2014; Yang et al., 2016). Thus, it is necessary to identify the specific values of K_c and K_{cb} across different agricultural ecosystems and environmental conditions, as these values provide important guidance for local irrigation practices and can be used to improve water-use efficiency (Yang et al., 2016). In addition, the relationships of both K_c and K_{cb} to various ecological and environmental factors (e.g., canopy conductance, leaf area index [*LAI*], and vapor-pressure deficit) need to be investigated in detail. However, as far as we know, such studies are relatively few.

To improve regional food security, China has been forced to implement cultivation in many areas where water is scarce. For example, the landscape in arid northwestern China is characterized by widely distributed gobi desert (i.e., desert with a gravel surface) interspersed with many oases, where there is abundant light to support agricultural ecosystems but limited water resources (Zhu et al., 2007, 2008, 2014). In this region, a phenomenon known as the "oasis effect", which involves evaporative cooling over areas of water that leads to advection of warmer bodies of air, is often observed on clear days (Wang and Mitsuta, 1992; Lee et al., 2004). Previous studies have indicated that the oasis effect will increase *ET* in agricultural systems (Prueger et al., 1996; Lei and Yang, 2010; Ding et al., 2015). However, fewer studies have attempted to investigate the impact of the oasis effect on K_c and its components in the arid oasis agricultural systems in northwestern China.

In the present study, direct measurements of the components of *ET* obtained by combining the sap flow and eddy-covariance techniques in a grapevine ecosystem in the arid region of northwestern China. Our main objectives were: (1) to investigate the seasonal variations of K_c, K_{cb}, and K_e under the advective conditions; (2) to identify the relationships of both K_c and K_{cb} to local ecological factors; and (3) to evaluate the impact of the "oasis effect" on K_c.

2. Materials and methods

2.1. Study sites

The experiment was conducted in a grapevine (*Vitis vinifera* cv. 'Thompson Seedless') ecosystem during the 2014 and 2015 growing seasons. The study site is located in the Nanhu Oasis of northwestern China (39°52′34″N, 94°06′19″E; 1300 m a.s.l.). One plot in an area of 7.2 ha (450 m × 160 m) was selected in this area to conduct our study. The canopy height of the vineyard was about 2.5 m above the ground (Fig. 1a, b). The planting pattern of the grapes was in rows, with a spacing of 3 m between rows and 1 m between grapes trellises (Fig. 1c), with the rows oriented from north to south. Weeds at the study site were removed regularly during the whole growth stage. Pruning was performed around DOY 230 during 2014 and 2015 to improve the yield and increase the water use efficiency. The root depth of the grapevines was about 2.0 m below the surface with about 1.5 m of the lateral root spread in the inter-row space, which was too shallow to reach the groundwater caused by the deep water table (10–50 m) in this region (Ma et al., 2013;). Therefore, the contribution of ground water was not considered in the computations. Plants received flood irrigation about every 20 days during the growth stages. Based on the FAO classification, the soil type is Arenosols, with a mean soil bulk density being 1.41 g cm^{-3} (Yan et al., 2015). The values of the measured field water capacity (θ_{FC}) at site was 0.28 m^3 m^{-3}, and the wilting point (θ_{WP}) by Allen et. al. (1998) was about 0.13 m^3 m^{-3}. The annual total solar

radiation ranged from 5903.4 to 6309.5 MW m^{-2}, which provided sufficient sunlight for grapes in the study area. The annual mean temperature and rainfall were 9.3 °C and 36.9 mm, respectively, with mean monthly temperatures ranging from -9.3 °C in January to 24.9 °C in July (Yan et al., 2015).

2.2. Eddy covariance and sap flow measurements

Eddy-covariance method was used to measure the daily *ET* in the grapevine field. The eddy-covariance instrumentations (Fig. 1e) were installed at 4.0 m above the ground level, which consist of an open-path H$_2$O & CO$_2$ analyzer (LI-7500, LI-Cor Inc., Lincoln, NE, USA), and a three-dimensional sonic anemometer (R3-50, Gill Instruments, UK). There were four soil heat flux plates (HFP01SC; Hukseflux, Netherlands) installed at a depth of 50 mm below the ground surface, soil heat flux (*G*) was calculated by averaging the four directions of heat fluxes data from sensors. Measurements were made continuously from 15 April (day of year [DOY] 105) to 13 October (DOY 285) in 2014 and 2015. The dominant wind direction during the study period was north-east. The 80% of contributing source area was from 150 m (stable stratification) to 250 m (unstable stratification), and the dominant direction was north-east, indicating the measured fluxes were primarily contributed by the vineyard (Fig. 1b). All data were recorded at a frequency of 10 Hz using a data logger (CR1000, Campbell Scientific, Logan, UT, USA), and the average value of 30 min was computed, daily averages were calculated during post-processing. Linear interpolation method was used to complete daily ET values when the data gaps were less than 2 h in a day. Any day that did not have necessary measurements to complete a diurnal cycle were discarded in this study. In addition, observations during the rainfall events were not used as the eddy covariance measurements were less reliable during precipitation events (Zhao et al., 2015; Yang et al., 2016).

The energy-balance closure method, which is based on conservation of energy, was used to evaluate the quality of eddy covariance data. Fig. 2 shows strong and statistically significant fits for the energy-balance closure (slopes = 0.91 and 0.87 with R^2 = 0.82 and 0.87 in 2014 and 2015, respectively), which was comparable to that in previous studies conducted in vineyards under similar circumstances (Ferreira et al., 2012). Generally, between 10% and 30% of the energy was missing from the energy balance as being common in previous research (Oncley et al., 2007; Foken, 2008; Allen et al., 2011). The results suggest that the energy-balance closure in present study was reasonable. Meanwhile, to overcome the issue of energy imbalance, the Bowen ratio method was applied to correct the measured *ET*, and the results could be seen in Supplement.

Sap-flow measurements were made from 1 May (DOY 121) to 13 October (DOY 285) in 2014, and between 21 June (DOY 172) and 13 October (DOY 285) in 2015.Six grapevines that covered the whole range of diameters were selected each year, with their diameters at breast height ranging from 2.01 to 4.14 cm. Sap flow (*F*, g h^{-1}) was measured using a Flow 32A-1 K system (Dynamax, Austin, TX, USA) according to the heat-balance method (Sakuratani, 1981). The probes were mounted more than 40 cm above the ground on the grapevine's trunk to avoid damage from the irrigation water, and were wrapped in aluminum foil to minimize the effects of solar heating (Fig. 1d). Details of the installation and the theory behind the measurements were provided by Trambouze and Voltz (2001).

2.3. Other variables

Weather variables were measured at the study site using an automatic weather station. The global solar radiation was observed at a height of 3 m above the soil surface (NR01; Hukse Flux, Delft, the Netherlands). Both *RH* and air temperature (HMP60, Vaisala, Helsinki, Finland) were monitored at heights of 3.0, 2.5, 2.0, 1.5, and 1.0 m above the soil surface. The CR1000 data logger was used to store and
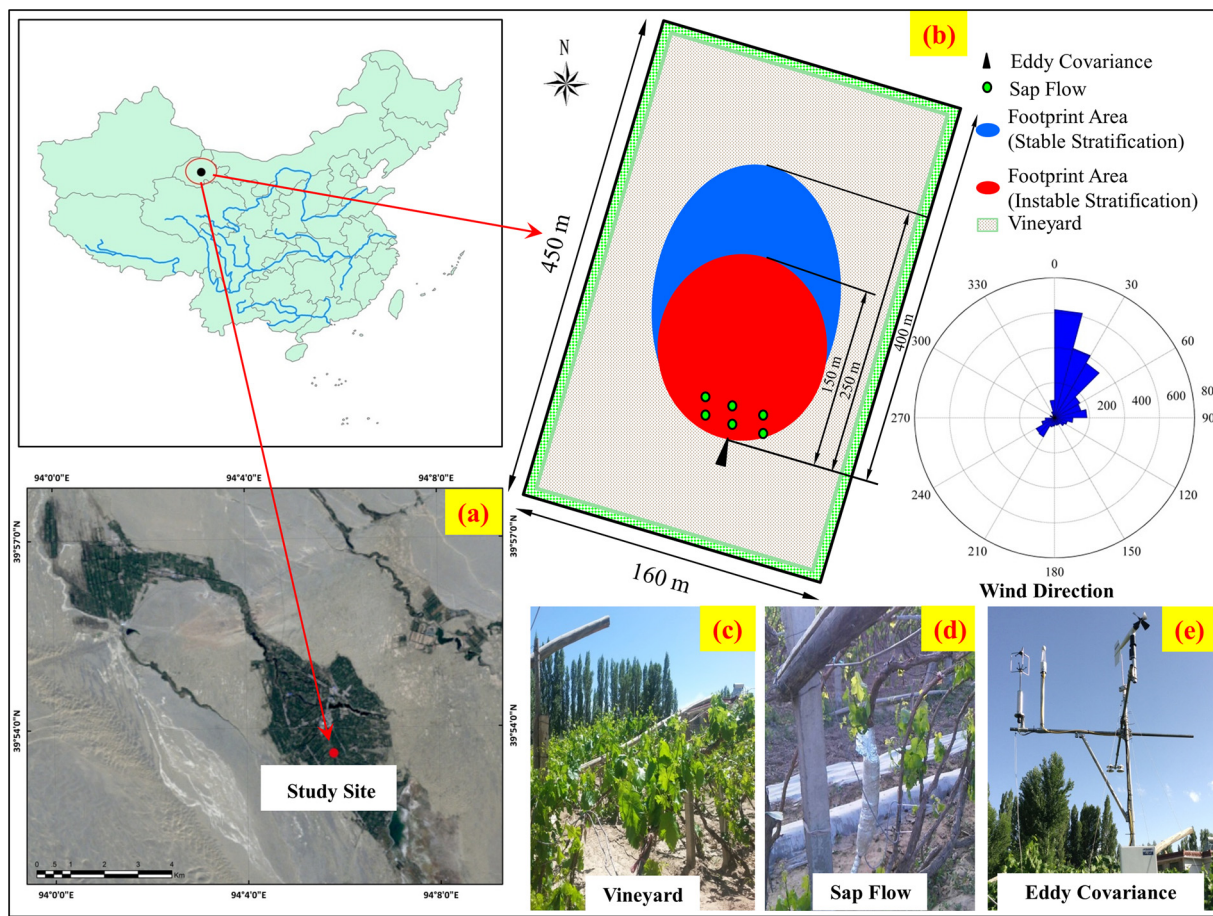
Fig. 1. (a) Location of the study site in Gansu Province, northwestern China. (b) The flux footprint area of the study site. (c) Image of the vineyard and soil surface. (d) Sap flow measurements. (e) Equipment used for both eddy covariance and meteorological measurements.

compute the half-hourly means of these data. Volumetric water content (*VWC*) at 5, 10, 20, 50, 80 and 100 cm depths was measured continuously during two study periods (ML2x, Delta T, UK).

An LAI-2200C plant canopy analyzer (Li-Cor) was used to measure the canopy *LAI*. A regression relationship was defined between leaf area (*LA*, cm^2) and the leaf width (*LW*, cm) and leaf length (*LL*, cm): $LA = 0.70\ LW \times LL + 2.57$ ($R^2 = 0.98$). 200 leaves were collected from the grapevines in the study plot to obtain this regression

relationship. The total leaf area (*A*, m^2) was calculated from the measurements of all leaves for each sample grapevine.

2.4. Parameter calculations

The half-hourly canopy transpiration (*T*; mm h^{-1}) was computed as follows (Yan et al., 2015; Soegaard and Boegh, 1995).
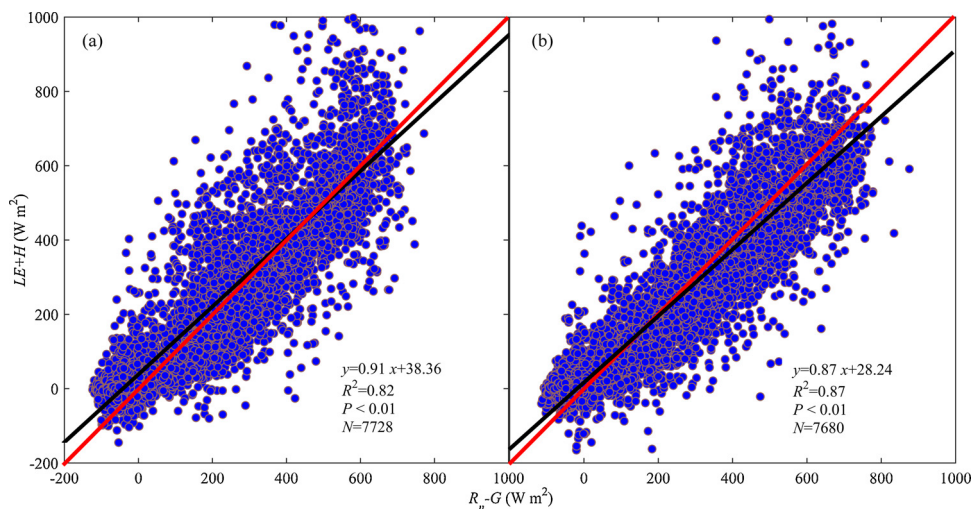

Fig. 2. Half-hour period energy-closure balance regressions analysis during the growing periods in (a) 2014 and (b) 2015. Variables: *G*, heat flux from the ground; *H*, sensible heat; *LE*, latent heat; *R*$_n$, net radiation, Black lines represent the regression equations; red lines represent *y* = *x*.

$$T = \frac{k}{N} \sum_{i=1}^{N} \frac{F_i}{A_i} \times LAI \tag{1}$$

where N is the number of samples; $k = 0.001$; F_i is the sap flow in sample i (g h^{-1}); A_i is the leaf area of sample i (m^2). The daily canopy transpiration (T; mm d^{-1}) was calculated by summing the half-hourly T values from Eq. (1).

Three crop coefficients (K_c, K_{cb}, and K_e) for the grapevines were calculated as follows (Allen et al., 1998):

$$K_c = \frac{ET}{ET_0} \tag{2}$$

$$K_c = K_{cb} + K_e \tag{3}$$

$$K_{cb} = \frac{T}{ET_0} \tag{4}$$

where K_c is the overall crop coefficient, K_{cb} is the portion of K_c accounted for by transpiration (T); K_e is the portion of K_c accounted for by soil evaporation (E); ET is the measured evapotranspiration; and ET_0 (mm d^{-1}) is the daily reference evapotranspiration, which is calculated using the standardized Penman-Monteith equation (Jensen et al., 1990; Allen et al., 1998).

The analysis was only conducted under good water status conditions due to the definition of K_c (Allen et al., 1998). That is, when the water stress coefficient (K_s) was less than 1 during two study periods, corresponding observations were discarded (see details in Supplement). Therefore, the K_c and K_{cb} values used in present study represent conditions without water stress. The K_c during the middle ($K_{c\text{-mid}}$) and late ($K_{c\text{-late}}$) growth stages is usually adjusted using the FAO-56 method when U_2 (the wind speed at a height of 2 m) is not equal to 2.0 m s^{-1} and RH_{min} (the average value of the minimum daily RH (%) during the middle and late stages of growth) is different from 45% (Allen et al., 1998). The adjustment equations are expressed as follows:

$$K_{c\text{-mid}} = K_{c\text{-mid(Tab)}} + [0.04 \times (U_2 - 2) - 0.04 \times (RH_{min} - 45)] \times (\frac{h}{3})^{0.3} \tag{5}$$

$$K_{c\text{-late}} = K_{c\text{-late(Tab)}} + [0.04 \times (U_2 - 2) - 0.04 \times (RH_{min} - 45)] \times (\frac{h}{3})^{0.3} \tag{6}$$

where $K_{c\text{-mid(Tab)}}$ and $K_{c\text{-late(Tab)}}$ are the corresponding mid-season and late-season values, respectively, under standard conditions that were provided in Table 12 of the FAO-56 method (Allen et al., 1998); and h is the average crop height at the corresponding stages (m). A similar approach was used to adjust the values of $K_{cb\text{-mid}}$ and $K_{cb\text{-late}}$ for the transpiration components during the middle and late stages (respectively) of the growing season.

The grapevine growth stages were classified as initial, development, middle season, and late season based on the FAO-56 segmentation approach (Allen et al., 1998). Horizontal line segments were used to represent the growth curve during the initial and middle parts of the season, but used increasing and decreasing line segments to represent the development and late parts of the season, respectively.

Canopy conductance (G_c; mm s^{-1}) was expressed as follows (Jarvis et al., 1986; Monteith and Unsworth, 1990):

$$G_c = \frac{\lambda T \gamma(Ta)}{\rho(Ta)C_\rho VPD} \tag{7}$$

where λ is the latent heat of vaporization of water (J kg^{-1}), T is transpiration (kg m^{-2} s^{-1}), $\gamma(T_a)$ is the psychrometric constant (as a function of air temperature [T_a], kPa K^{-1}), $\rho(T_a)$ is the density of liquid water at temperature T_a (kg m^{-3}), C_p is the specific heat of air (J kg^{-1} K^{-1}), and VPD is the vapor-pressure difference between the leaf interior and the atmosphere (kPa).

The daily R_{ad}, which represents the contribution of K_c from advection (oasis effect), was calculated as follows (McNaughton, 1976; Smith et al., 1997; Ding et al., 2015):

$$R_{ad} = \frac{(ET - ET_{eq})/ET_0}{ET/ET_0} \tag{8}$$

where ET_{eq} was calculated according to the method of McNaughton and Jarvis (1983), as follows:

$$ET_{eq} = \frac{\Delta}{\Delta + \gamma}(R_n - G) \tag{9}$$

where R_n is the net radiation (MJ m^{-2} d^{-1}); G is the soil heat flux (MJ m^{-2} d^{-1}); and Δ is the slope of the vapor-pressure curve (kPa °C^{-1}).

2.5. Statistical analysis

The Normalized root mean square error (NRMSE) and mean absolute error (MAE) were used to evaluate the performance of the dual-K_c approach.

$$NRMSE = \frac{1}{\overline{Y}} \sqrt{\frac{1}{N} \sum_{i=1}^{N} (X_i - Y_i)^2} \tag{10}$$

$$MAE = \frac{1}{N} \sum_{i=1}^{N} |X_i - Y_i| \tag{11}$$

where N is the number of observations, X_i and Y_i are estimated and observed values, respectively, $\overline{Y}$ is the averaged value of observations.

3. Results and discussion

3.1. Environmental and ecological factors

Variations of daily physiology and environmental conditions during different growth stages in 2014 and 2015 were presented in Fig. 3, including the maximum, minimum and average daily air temperature (T_a; °C), the daily reference evapotranspiration (ET_0; mm d^{-1}), volumetric water content (VWC; m^3 m^{-3}), rainfall ($Rain$; mm), average daily relative humidity (RH; %), vapor pressure deficit (VPD; kPa), average daily wind speed (u; m s^{-1}), leaf area index (LAI; m^2 m^{-2}), canopy conductance (G_c; mm s^{-1}) and irrigation amounts (I; cm). There were no considerable seasonal differences between two experimental years. The daily air temperature (T_a) varied from -4.02 to 36.93 and -2.57 to 38.25 °C with an average value of 18.52 and 18.89 °C during experimental periods in two years, respectively (Fig. 3a and b). The daily ET_0 varied from 0.80 to 7.11 and 1.13 to 7.32 mm d^{-1} with an average value of 3.73 and 4.28 mm d^{-1} during experimental periods in two years, respectively (Fig. 3a and b). The total precipitation was 13.2 mm in 2014 and 50.8 mm (with four events greater than 5.0 mm) in 2015 (Fig. 3c and d). VWC has a wide range over the whole growing season, and the variability of VWC was mainly depended on local irrigation scheduling and rain (Fig. 3c and d). The peak value of VWC was reached after rain and irrigation (about 0.32 m^3 m^{-3}) and would gradually reduce until the next irrigation (rain). The average daily relative humidity (RH) ranged from 11.6 to 75.8% and from 10.3 to 90.6% in 2014 and 2015, respectively (Fig. 3e and f). Daily vapor pressure deficit (VPD) varied from 0.30 to 2.78 kPa and from 0.18 to 2.59 kPa in 2014 and 2015, respectively (Fig. 3e and f). Daily mean u ranged from 0.19 to 1.53 m s^{-1} and from 0.13 to 1.52 m s^{-1} during two experimental periods, respectively (Fig. 3g and h).

Detailed information on the main physiological variables is essential to evaluate the seasonal variation of K_c and its partitioning. In both years, LAI increased rapidly from the initial to the middle stage, and then decreased slowly thereafter. The peak LAI of 4.88 m^2 m^{-2} was reached on 22 August 2014 (DOY 234; Fig. 3g) and the peak of 4.67 m^2 m^{-2} was reached on 23 August 2015 (DOY 235; Fig. 3h). Daily G_c ranged from about 0.56 mm s^{-1} at the initial stage in both years to
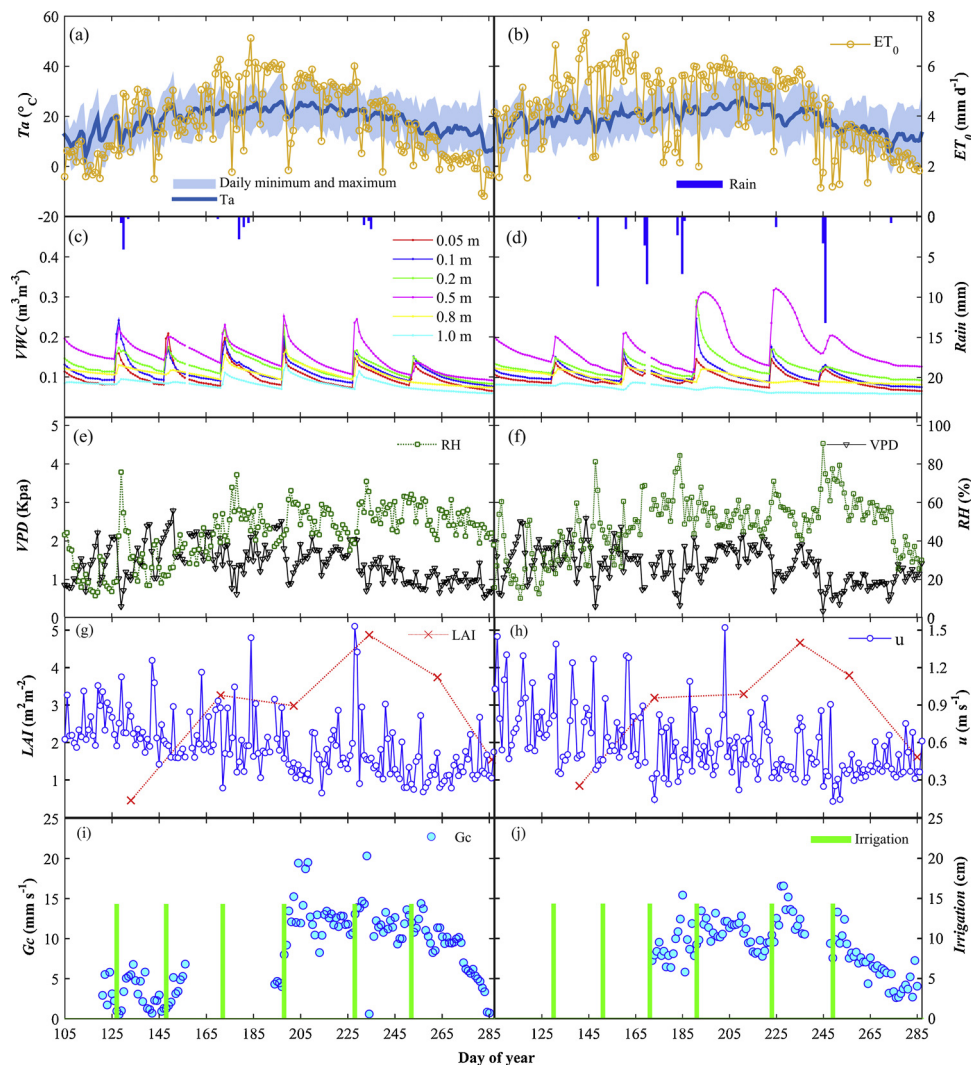
Fig. 3. Seasonal variation of environmental and ecological factors in 2014 (a, c, e, g, i) and 2015 (b, d, f, h, j) during the study periods, including daily average, minimum and the maximum temperature (T_a), daily reference evapotranspiration (ET_0), volumetric water content (VWC) at 0.05, 0.1, 0.2, 0.5, 0.8 and 1.0 m depth, rainfall ($Rain$), average daily relative humidity (RH), vapor pressure deficit (VPD), average daily wind speed (u), leaf area index (LAI), canopy conductance (G_c) and irrigation amounts (I).

$20.35 \, mm \, s^{-1}$ in 2014 and $16.60 \, mm \, s^{-1}$ in 2015 at the middle stage; thereafter, it declined to about 1.19 and $0.96 \, mm \, s^{-1}$ at the late stage in 2014 and 2015, respectively (Fig. 3i and j). In previous research, the highest value of daily G_c was $32.5 \, mm \, s^{-1}$ among primary vegetation types with an extensive LAI range (Kelliher et al., 1995). Thus, our results fall within the range reported from previous studies of daily G_c. Irrigation in both years was about 142.5 mm each time, at an interval of about 20 days.

3.2. Crop transpiration versus evapotranspiration

Fig. 4 shows the seasonal variations of ET and T during the growing seasons in 2014 and 2015. The transpiration data from DOY 157 to 193 in 2014, DOY 120 to 172 and DOY 238 to 245 in 2015 were missing due to the malfunctions of the instruments and power failures. The daily values of T increased from $0.09 \, mm \, d^{-1}$ during the initial stage of the growing season in 2014 (T value during the initial stage in 2015 was missing), to 7.52 and $7.07 \, mm \, d^{-1}$ (respectively) during the corresponding middle stages, and then decreased gradually until the leaf-fall season. Meanwhile, the ET values ranged from 0.80 and $0.99 \, mm \, d^{-1}$ during the initial stages of the growing season in 2014 and 2015, respectively, to 9.87 and $8.73 \, mm \, d^{-1}$ when the canopy reached full

cover, and then declined steadily until the leaf-fall season. The mean values of ET were 4.63 and $4.77 \, mm \, d^{-1}$ in 2014 and 2015, respectively, versus corresponding averages of 3.00 and $3.33 \, mm \, d^{-1}$ for T. These results were higher than those in previous studies of grapevines (Ortega-Farias et al., 2010; Picón-Toro et al., 2012; Poblete-Echeverría and Ortega-Farias, 2013). The high values of ET and T can be attributed to the high ET_0, combined with high LAI, and oasis effect at the study site.

The ratio of T/ET was 58.4% and 55.1% in 2014 and 2015, respectively. The results suggested that the crop transpiration (T) during the summer is a dominant water flux of evapotranspiration (ET) compared to others (Sutanto et al., 2014). Concomitantly, the T/ET ratios were lower than the values for grapevines under drip irrigation, which ranged from 78.9 ± 3.1% (mean ± SD) to 84.1 ± 1.3% (López-Urrea et al. (2012); Poblete-Echeverría and Ortega-Farias, 2013). In particular, Fandiño et al. (2012) suggested that the ratio of T/ET ranged from 85% to 92% under sub-drip irrigation at vineyards with active ground cover, and also, applying sub-drip irrigation and having active ground cover that highly contributed to the total transpiration (47% to 58% of total T). These could be interpreted by the fact that water use efficiency of drip irrigation was higher than that of flood irrigation. However, our results were greater than the values measured from
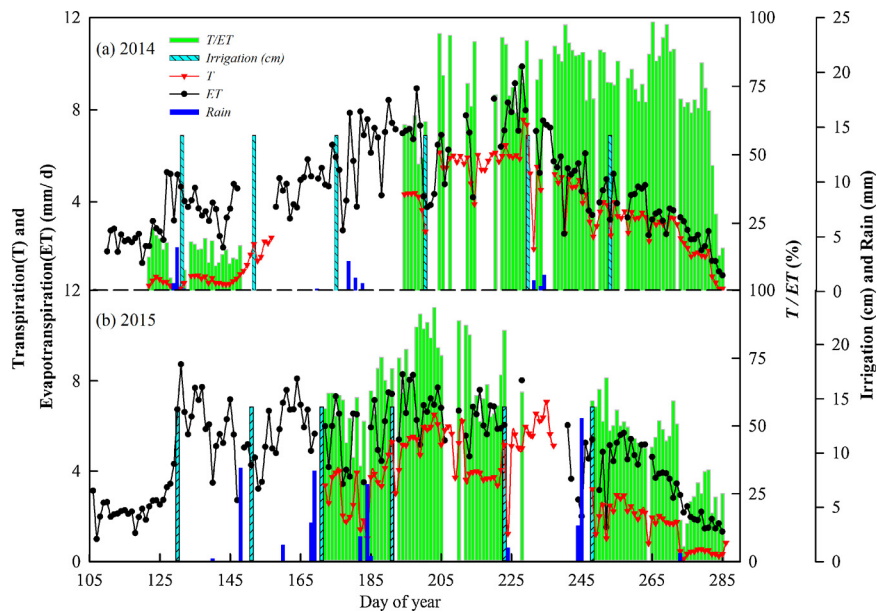
Fig. 4. Seasonal variations of canopy transpiration (*T*) and evapotranspiration (*ET*) and the value of the *T/ET* ratio in (a) 2014 and (b) 2015.
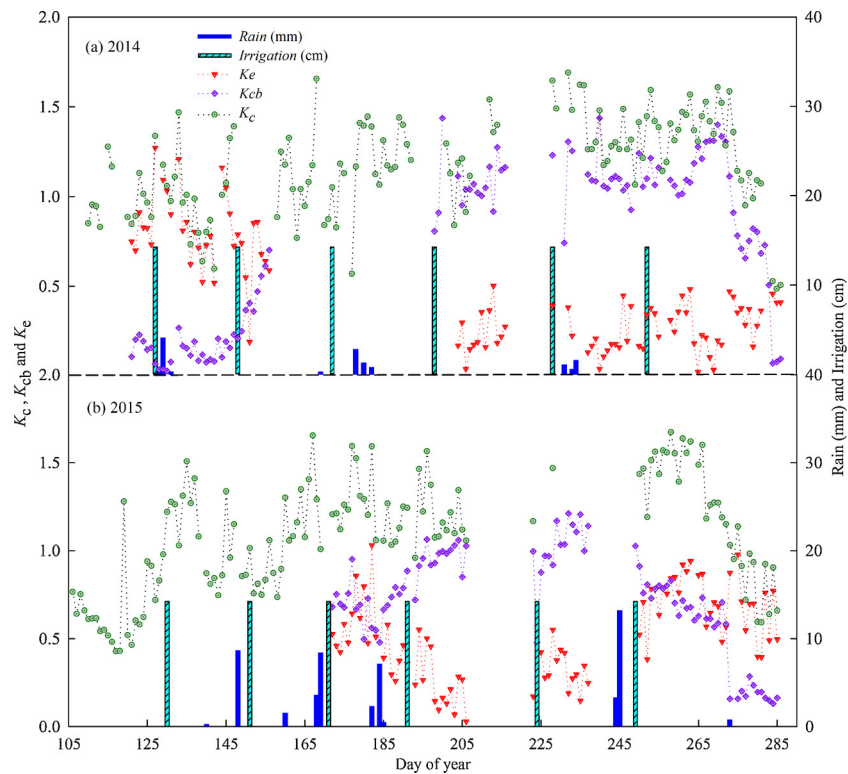

Fig. 5. Seasonal variations of the three crop coefficients (*K*$_c$, overall; *K*$_{cb}$, transpiration component; and *K*$_e$, evaporation component) in (a) 2014 and (b) 2015.

Table 1
Durations of the key growth stages for grapevines.

	Growth stage (duration, in days)				Total no. days
	Initial	Development	Middle	Late	
2014	21	64	75	20	180
2015	25	65	70	20	180
Average	23	65	72	20	180

vineyard with low fractional cover (50.7% ± 2.4%; Zhao et al., 2015). The small values of *T/ET* for vines with low fractional cover may be because the available energy intercepted by the canopy for transpiration was low during the growth stage. The differences between present study and previous results clearly indicated that the ratio of *T/ET* is strongly affected by water availability, ambient conditions, irrigation system, and canopy characteristics (Schlesinger and Jasechko, 2014). Therefore, locally specific estimates of the ratio were still needed.

Table 2
Values of crop coefficients for the local and FAO-56 climate adjusted values.

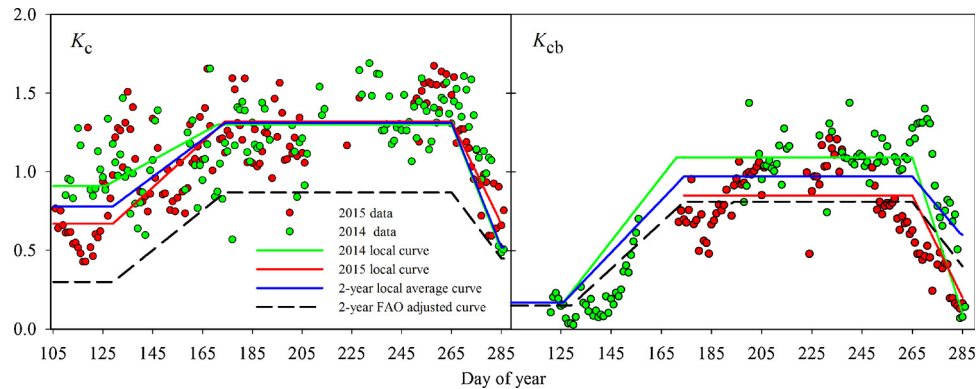|	2014			2015			Average			$K_{c\text{-FAO-adj}}$		
	initial	middle	late	initial	middle	late	initial	middle	late	initial	middle	late
K_c	0.91	1.30	1.16	0.67	1.32	0.99	0.79	1.31	1.08	0.30	0.87	0.47
K_{cb}	0.17	1.09	0.85	–	0.85	0.43	–	0.97	0.64	0.15	0.81	0.42

Fig. 6. K_c curves and curves for the transpiration component of K_c (K_{cb}) based on local data and the FAO-56 climate adjustments in 2014 and 2015.
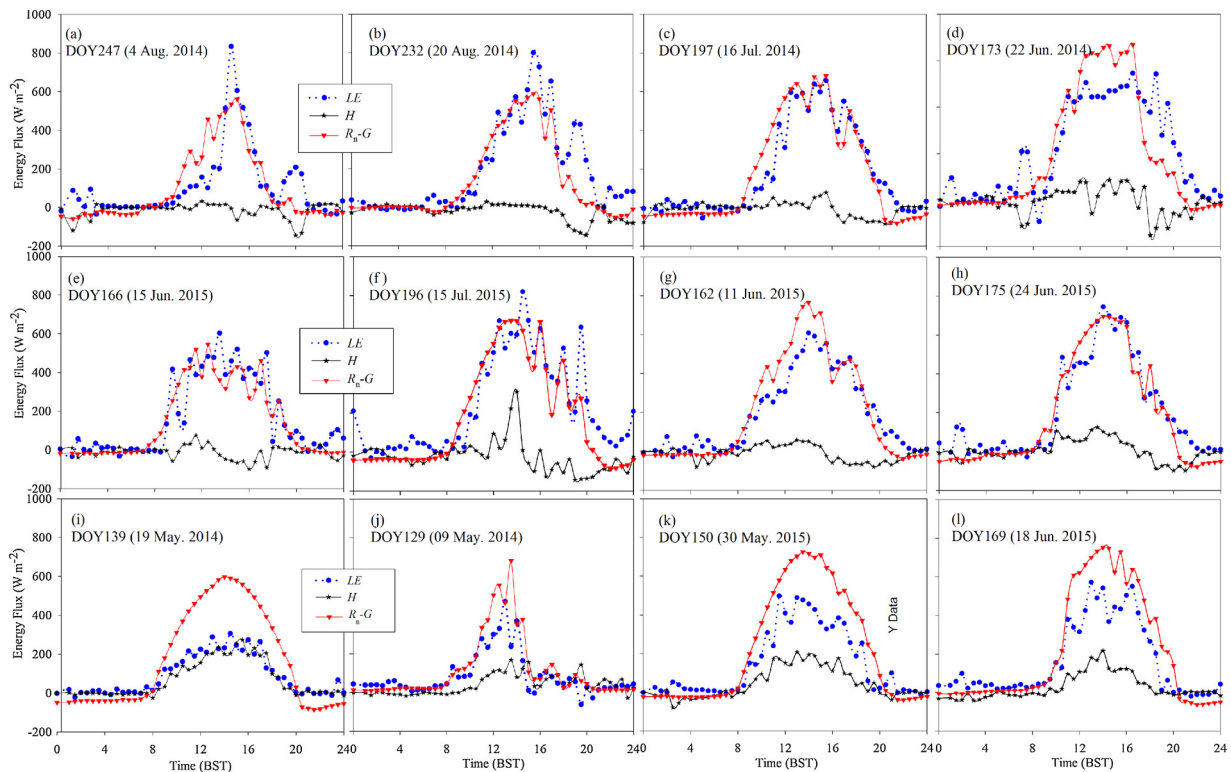

Fig. 7. Diurnal trends in the available energy (R_n-G), LE, and H at the study site; **(a–h):** Days when advection occurred; **(i, k):** Diurnal trend on a clear day without advection ; **(j, l):** Diurnal trend on a rainy day.

3.3. Local K_c and K_{cb} versus FAO-56 climate adjusted values

Seasonal variations of daily K_c and K_{cb} displayed similar tendency during two experimental years (Fig. 5). Daily values of K_c increased from nearly 0.45 during the initial stages to about 1.65 by the middle stages, and then gradually decreased. The K_{cb} values were also having the similar trend during the growth stage. At the same time, daily values of K_e demonstrated an approximately opposite trend during the 2014 and 2015 growing seasons. The highest values of K_c and K_{cb} generally appeared when the canopy reached its full expansion and the soil moisture was completely adequate, but the peak values of K_c and K_{cb} were generally transitory. Our results agree with those in a number of previous studies for grapes (Grimes and Williams, 1990; Williams et al., 2003a, b). The maximum seasonal value of K_c in the present study was in excess of 1.0, which was comparable to those reported in previous studies. For example, Johnson et al. (2005) suggested the maximum K_c values were between 1.10 and 1.20 in an American vineyard. Allen and Pereira (2009) provided a peak K_c of 1.10 for grapes during the middle season. Netzer et al. (2009) reported a peak K_c of 1.20 for grapevines (*V. vinifera* cv. 'Superior Seedless') in southern Israel. Picón-
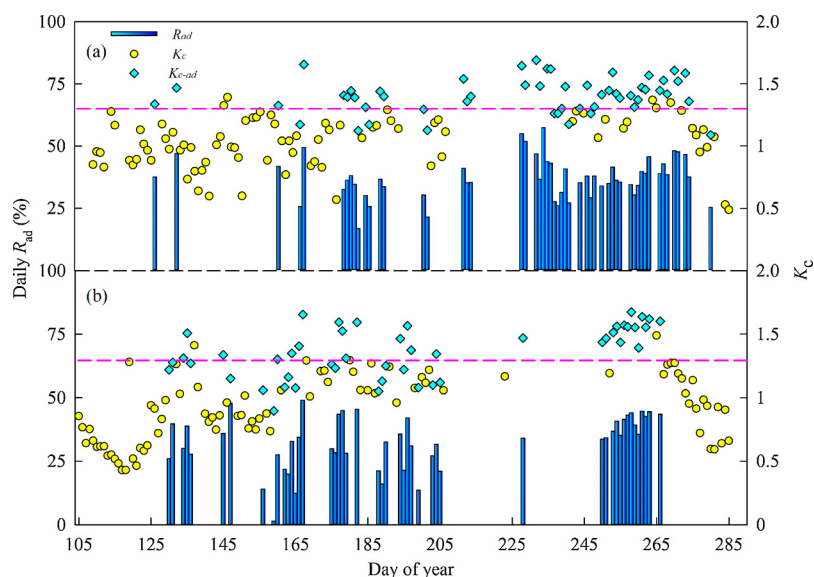
Fig. 8. Seasonal trends in the daily R_{ad} at the study site on clear days during the study periods in (a) 2014 and (b) 2015.
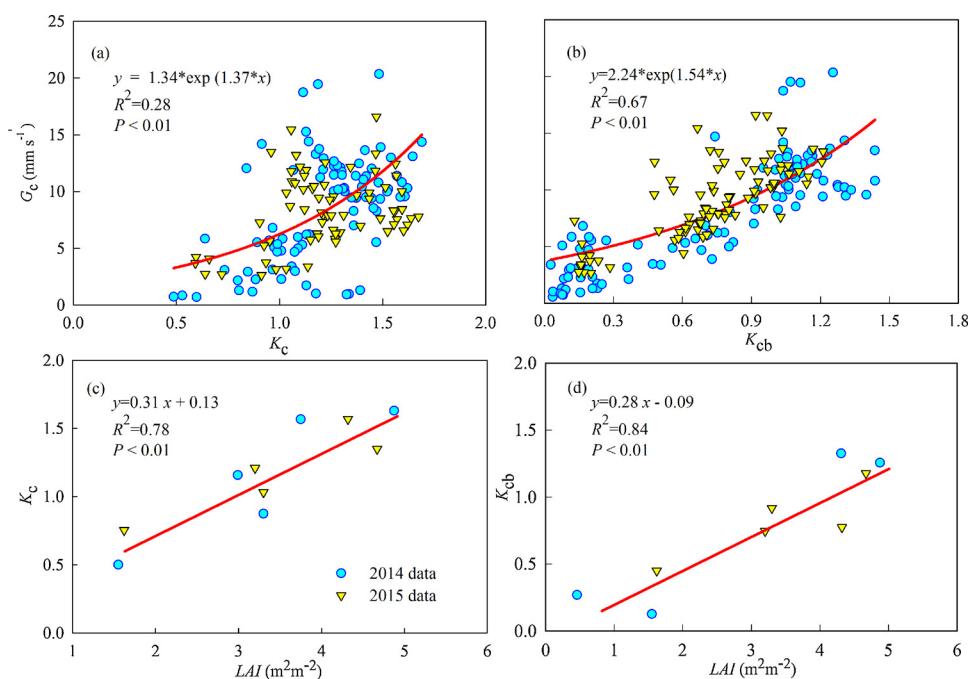

Fig. 9. Relationships between the crop coefficients (K_c and K_{cb}) to **(a–b)** G_c and *LAI* **(c–d).**

Toro et al. (2012) reported the maximum value of K_c was close to 2 for "Tempranillo" during their study periods in south-western Spain. The differences among these studies in the maximum K_c value probably resulted from uncertainties in the calculation method, combined with the use of different cultivars, different irrigation methods, and different environmental conditions.

Table 1 shows the observed durations of the growth stages during the two study periods. This, combined with other factors, leads to differences between the local observed K_c ($K_{c\text{-Local}}$) and the FAO-56 climate adjusted K_c ($K_{c\text{-FAO}}$) for the growth stages (Table 2, Fig. 6). Table 2 indicates that the average observed K_c was higher than $K_{c\text{-FAO}}$ in both study periods. After examining the possible reasons for the higher K_c values in the present study, we hypothesize that the increased T and E that result from higher solar radiation and temperature were, by themselves, insufficient to cause the remarkable increase of K_c because the E value would be relatively low when the canopy reached its

maximum coverage, even when combined with high levels of solar radiation and high temperatures (Allen et al., 1998). Thus, it was necessary to determine what other factors could have contributed to the increased K_c.

One possibility is the oasis effect (Rosenberg et al., 1983; Prueger et al., 1996; Zhu et al., 2014), which could result from high surface heterogeneity. This was often observed during cloud-free days at our study site, when the sensible heat flux (H) was close to zero or even negative near ground level due to the advection of hotter air from the surrounding desert areas, causing a flow of warm air to the study site (Li and Yu, 2007; Lei and Yang, 2010; Zhu et al., 2014). At the same time, the latent heat (LE) often equaled or exceeded the local available energy (net radiation minus the heat flux from the ground; R_n-G) due to the downward fluxes of H as energy inputs into the ET processes (Evett et al., 2012; Zhu et al., 2014). To examine the contribution of the oasis effect to K_c, five clear days and one rainy day in 2014 and 2015 were
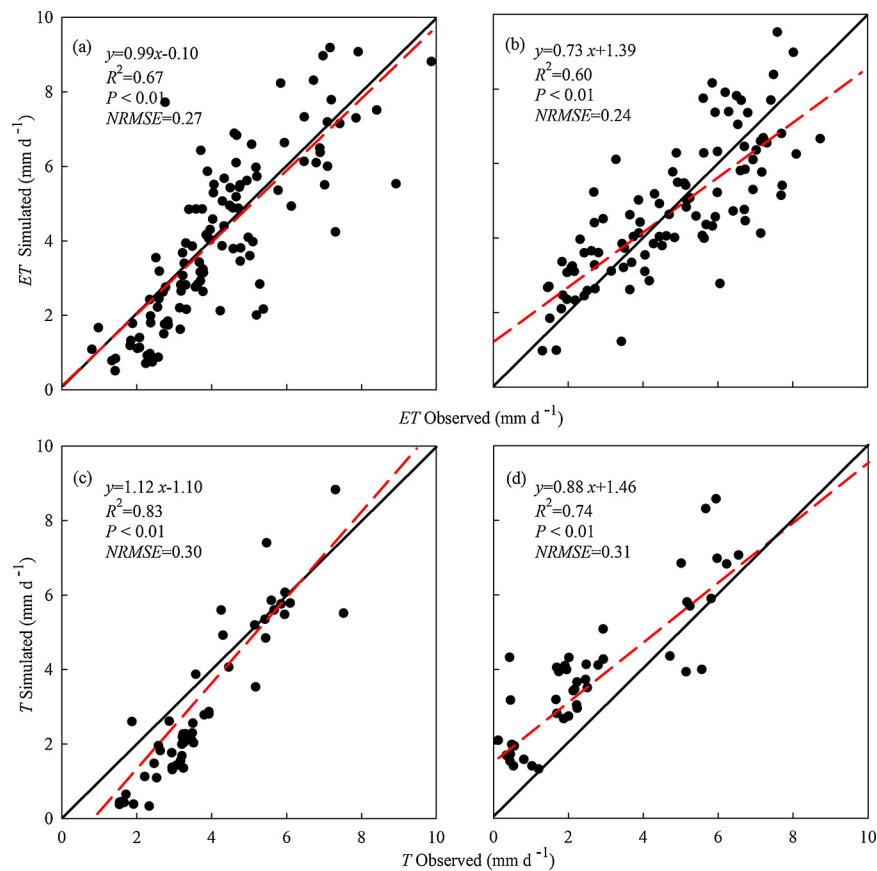
Fig. 10. Cross-validation for the relationships between the daily observed and simulated values of (a,b) evapotranspiration (*ET*) and (c,d) transpiration (*T*) based on data from throughout the growing season for the grapevines in (a, c) 2014 and (b, d) 2015. Red lines represent the regression equations; black lines represent $y = x$.

chosen to investigate the possibility of heat advection (Prueger et al., 1996; Zhu et al., 2014). Fig. 7 a–h shows that on clear days, a prominent advection process could be detected at 14:00 (13:00), 14:30 (14:30), 15:30 (15:30), and 16:30 (16:30) BST (Beijing standard time) in 2014 (2015), respectively, which suggested that the sensible heat flux (*H*) provided the energy that drove *ET* evapotranspiration in the vineyard during the period surrounding these times. In contrast, days when advection was absent happened sometimes during days with a clear sky in 2014 (Fig. 7i) and 2015 (Fig. 7k), and during a rainy day in 2014 (Fig. 7j) and 2015 (Fig. 7l).

Fig. 8 shows the dynamics of daily R_{ad} during the 2014 and 2015 study periods. R_{ad} could be positive or negative for a given day during the study period, which demonstrates that the oasis effect can either increase or decrease K_c. All the days during the two study periods showed obviously positive R_{ad}, suggesting that the oasis effect increased K_c when positive advection occurred because *H* afforded the energy for *ET* rather than consumption of available energy. The contribution of the oasis effect to K_c ranged from 16.9% to 57.4% in 2014 and from 1.4% to 49.0% in 2015, indicating that the oasis effect contributed substantially to the crop coefficient (K_c). Our estimates of this contribution were higher than those in a previous study in cropland (4.4–28.0) (Ding et al., 2015), but comparable to the sensible heat advection achieved in previous studies under a similar environment (> 50.0%) (Li and Yu, 2007). Therefore, the effects of the oasis effect on daily K_c should not be ignored in future research. In general, the use of irrigation in farmland will generate the oasis effect, thereby increasing daily K_c, so accounting for the influence of this effect on K_c could help managers modify their irrigation practices to reduce water consumption (Ding et al., 2015).

3.4. Effects of physiological factors on K_c and K_{cb}

Fig. 9 illustrates the relationships between the two crop coefficients (K_c, K_{cb}) and the main factors that influence them. The relationships between the crop coefficients (K_c, K_{cb}) and *LAI* were moderately strong and statistically significant ($R^2 \geq 0.78$, $P < 0.01$) in both years (Fig. 9 a–b), which agrees with previous results by Williams and Ayars (2005) for grapevines ('Thompson Seedless') in California. Intrigliolo et al. (2009) also found a significant relationship, with an average K_{cb} of 0.49 in grapevines ('Riesling') at *LAI* = 1.57, which was comparable to the present results. These similarities suggested that the relationships between the crop coefficients and *LAI* could be applicable for many different grape cultivars despite differences in the climate, varieties, datasets, and management system (Ding et al., 2015; Picón-Toro et al., 2012). Meanwhile, it seems that both K_c and K_{cb} to G_c was an exponential regression during two study periods (Fig.9c–d). In addition, *LAI* seems better able than G_c ($R^2 \leq 0.67$) to predict the crop coefficients in both years. Moreover, both *LAI* and G_c had a better fit with K_{cb} than with K_c, suggesting that *LAI* and G_c are likely to indicate *T* more accurately than *ET*. Therefore, K_{cb} may be more strongly affected than K_c by the physiological responses of grapevines to their cultivation environment.

3.5. Comparisons of observed and estimated ET and T values

Fig. 10 shows the results of a cross-validation between the daily measured and estimated values of *ET* and *T*, which can be used to evaluate the performance of the K_c and K_{cb} values estimated by means of the dual-K_c approach. The regression between the measured and estimated values of daily *ET* in both years was not statistically different from line 1:1, with R^2 being 0.67 and 0.60 in 2014 and 2015 (Figs.10a

and 10b), respectively. The normalized root mean square error (*NRMSE*) and mean absolute error (*MAE*) were 0.27 and 0.98 mm d^{-1} and 0.24 and 1.01 mm d^{-1} for 2014 and 2015, respectively. This agrees with the results of a previous study using the dual-K_c approach (Poblete-Echeverría and Ortega-Farias, 2013; Zhao et al., 2015). Our results therefore suggested that the values of K_c calculated by means of the dual-K_c method can provide a good estimate of the daily values of *ET*.

In contrast, the dual-K_c method seemed to slightly overestimating daily *T* in 2014, with the values of R^2, *NRMSE* and *MAE* being 0.83, 0.30 and 0.99 mm d^{-1}, respectively (Fig.10c). Nevertheless, it tended to slightly underestimate the daily values of *T* in 2015 with R^2, *NRMSE* and *MAE* being 0.80, 0.31 and 1.29 mm d^{-1}, respectively (Fig.10d). This resulted in some discrepancies between the strengths of the relationships between observed and simulated *T*. The discrepancies may be attributable to the uncertainty when scaling up *T* from individual trees to canopy scale. Meanwhile, the soil characteristics (e.g.θ_{FC}) measured at limited points may not adequately stand for the whole study site, and this can also contribute to some uncertainties in estimating *T* (Zhao et al., 2015). However, although the use of other models may overcome the uncertainties in estimating *ET* and *T*, our results nonetheless suggest that the dual-K_c methodologycould be used for providing acceptable daily *ET* and *T* estimates.

4. Conclusions

Our 2-year study of irrigated grapes in an arid region of northwestern China revealed the importance of regionally calibrated crop coefficients. The high values of *ET* and *T* can be attributed to the high ET_0, combined with high *LAI* and oasis effect. The values of the *T/ET* ratio were strongly affected by water availability, ambient conditions, irrigation system, and canopy characteristics. The average observed K_c was higher than $K_{c\text{-FAO}}$ in both study periods. The contribution of the oasis effect to daily K_c was too important to ignore in arid regions such as our study area. *LAI* is a better indicator than G_c when it was used to predict K_c and K_{cb}. The dual-K_c method let us estimate K_c and K_{cb} with good accuracy in the irrigated vineyard; as a result, it was possible to estimate *ET* and *T* with reasonable accuracy and account for inter-annual variability. Moreover, the local values of K_c and K_{cb} calculated by means of the dual-K_c methodology will improve real-time management of irrigation efficiency and improve water allocation under the regional environmental conditions, since water is a rare and precious resource in the study area.

Limitations still exist when measuring *T* and *ET* using *SF* and *EC* techniques. For some instances, uncertainty is generally produced when *SF* method is used to scale up *T* from individual trees to landscape. Meanwhile, although the EC techniques are widely used under a variety of conditions, the energy closure problem still exists. Thus, some other methods in estimating *ET* and *T* should be investigated in the future studies, such as *ET* models based on remote sensing observations or others based on Penman-Monteith equations. Although the relationships described in this paper were moderately strong, there was clearly room for improvement, particularly with respect to eliminating periods when the instruments were unavailable, leading to long periods with missing data.

Acknowledgments

Appendix A. Supplementary data

Supplementary material related to this article can be found, in the online version, at doi:https://doi.org/10.1016/j.agwat.2018.09.023.

References

Allen, R.G., Pereira, L.S., 2009. Estimating crop coefficients from fraction of ground cover and height. Irrig. Sci. 28 (1), 17–34.

Allen, R.G., Pereira, L.S., Raes, D., Smith, M., 1998. Crop Evapotranspiration Guidelines for Computing Crop Water Requirements. FAO Irrigation and Drainage Paper No. 56. FAO, Rome, Italy.

Allen, R.G., Pereira, L.S., Howell, T.A., Jensen, M.E., 2011. Evapotranspiration information reporting: i. Factors governing measurement accuracy. Agric. Water Manage. 98 (6), 899–920.

Campbell, D.N., Na, C.I., Rowland, D.L., Schnell, R.W., Ferrell, J.A., Wilkie, A.C., 2015. Development of a regional specific crop coefficient (kc) for castor (Ricinus communis L.) in Florida, USA by using the sap flow method. Ind. Crops Prod. 74, 465–471.

Cavanaugh, M.L., Kurc, S.A., Scott, R.L., 2011. Evapotranspiration partitioning in semi-arid shrubland ecosystems: a two-site evaluation of soil moisture control on transpiration. Ecohydrology 4 (5), 671–681.

Ding, R., Tong, L., Li, F., Zhang, Y., Hao, X., Kang, S., 2015. Variations of crop coefficient and its influencing factors in an arid advective cropland of northwest China. Hydrol. Process. 29 (2), 239–249.

Dirmeyer, P.A., Gao, X., Zhao, M., Guo, Z., Oki, T., Hanasaki, N., 2006. GSWP-2: multi-model analysis and implications for our perception of the land surface. Bull. Am. Meteorol. Soc. 87 (10). https://doi.org/10.1175/BAMS-87-10-1381.

Evett, S.R., Kustas, W.P., Gowda, P.H., Anderson, M.C., Prueger, J.H., Howell, T.A., 2012. Overview of the bushland evapotranspiration and agricultural remote sensing experiment 2008 (bearex08): a field experiment evaluating methods for quantifying et at multiple scales. Adv. Water Resour. 50 (6), 4–19.

Fandiño, M., Cancela, J.J., Rey, B.J., Martínez, E.M., Rosa, R.G., Pereira, L.S., 2012. Using the dual-kc approach to model evapotranspiration of albariño vineyards (*Vitis vinifera* L. cv. albariño) with consideration of active ground cover. Agric. Water Manage. 112, 75–87.

Ferreira, M.I., Silvestre, J., Conceição, N., 2012. Crop and stress coefficients in rainfed and deficit irrigation vineyards using sap flow techniques. Irrig. Sci. 30 (5), 433–447.

Flumignan, D.L., Faria, R.T.D., Prete, C.E.C., 2009. Evapotranspiration components and dual crop coefficients of coffee trees during crop production. Bragantia 68 (1), 269–278.

Foken, T., 2008. The energy balance closure problem: an overview. Ecol. Appl. 18 (6), 1351–1367.

Grimes, D.W., Williams, L.E., 1990. Irrigation effects on plant water relations and productivity of Thompson seedless grapevines. Crop Sci. 30 (2), 255–260.

Herbst, M., Kappen, L., Thamm, F., Vanselow, R., 1996. Simultaneous measurements of transpiration, soil evaporation and total evaporation in a maize field in northern Germany. J. Exp. Bot. 47 (12), 1957–1962.

Intrigliolo, D.S., Lakso, A.N., Piccioni, R.M., 2009. Grapevine cv.' Riesling' water use in the northeastern United States. Irrig. Sci. 27 (3), 253–262.

Jagtap, S.S., Jones, J.W., 1989. Stability of crop coefficients under different climate and irrigation management practices. Irrig. Sci. 10 (3), 231–244.

Jarvis, P.G., McNaughton, K.G., 1986. Stomatal control of transpiration: scaling up from leaf to region. Adv. Ecol. Res. 15 (15), 1–49.

Jasechko, S., Sharp, Z.D., Birks, S.J., Yi, Y., Fawcett, P.J., 2013. Terrestrial water fluxes dominated by transpiration. Nature 496 (7445), 347–350.

Jensen, M.E., Burman, R.D., Allen, R.G., 1990. Evapotranspiration and Irrigation Water Requirements: a Manual. American Society of Civil Engineers, Reston, VA.

Johnson, R.S., Williams, L.E., Ayars, J.E., Trout, T.J., 2005. Weighing lysimeters aid study of water relations in tree and vine crops. Calif. Agric. 59 (2), 133–136.

Jung, M., Reichstein, M., Ciais, P., Seneviratne, S.I., Sheffield, J., Goulden, M.L., et al., 2010. Recent decline in the global land evapotranspiration trend due to limited moisture supply. Nature 467 (7318), 951–954.

Kelliher, F.M., Leuning, R., Raupach, M.R., Schulze, E.-D., 1995. Maximum conductances for evaporation from global vegetation types. Agric. For. Meteorol. 73 (1-2), 1–16.

Kool, D., Agam, N., Lazarovitch, N., Heitman, J.L., Sauer, T.J., Bengal, A., 2014. A review of approaches for evapotranspiration partitioning. Agric. For. Meteorol. 184 (1), 56–70.

Lee, X., Qiang, Y., Sun, X., Liu, J., Min, Q., Liu, Y., et al., 2004. Micrometeorological fluxes under the influence of regional and local advection: a revisit. Agric. For. Meteorol. 122 (1-2), 111–124.

Lei, H., Yang, D., 2010. Inter-annual and seasonal variability in evapotranspiration and energy partitioning over an irrigated cropland in the North China Plain. Agric. For. Meteorol. 150 (4), 581–589.

Li, L., Yu, Q., 2007. Quantifying the effects of advection on canopy energy budgets and water use efficiency in an irrigated wheat field in the North China Plain. Agric. Water Manage. 89 (1–2), 116–122.

López-Urrea, R., Montoro, A., Mañas, F., López-Fuster, P., Fereres, E., 2012. Evapotranspiration and crop coefficients from lysimeter measurements of mature 'tempranillo' wine grapes. Agric. Water Manage. 112 (112), 13–20.

Ma, J., He, J., Qi, S., Zhu, G., Zhao, W., Edmunds, W.M., et al., 2013. Groundwater recharge and evolution in the Dunhuang Basin, northwestern China. Appl. Geochem. 28 (28), 19–31.

Marsal, J., Girona, J., Casadesus, J., Lopez, G., Stöckle, C.O., 2013. Crop coefficient (k$_c$) for apple: comparison between measurements by a weighing lysimeter and prediction by CropSyst. Irrig. Sci. 31 (3), 455–463.

McNaughton, K.G., 1976. Evaporation and advection I: evaporation from extensive homogeneous surfaces. Q. J. R. Meteorolog. Soc. 102 (431), 181–191.

McNaughton, K.G., Jarvis, P.G., 1983. Chapter 1–predicting effects of vegetation changes on transpiration and evaporation. Adv. Ecol. Res. 7 (2), 1–47.

Monteith, J.L., Unsworth, M.H., 1990. Principles of Environmental Physics. Edward

Arnold, London.

Netzer, Y., Yao, C., Shenker, M., Bravdo, B.A., Schwartz, A., 2009. Water use and the development of seasonal crop coefficients for superior seedless grapevines trained to an open-gable trellis system. Irrig. Sci. 27 (2), 109–120.

Oleson, K.W., Dai, Y.J., Bonan, G.B., Bosilovich, M., Dickinson, R.E., Dirmeyer, P., et al., 2004. Technical description of the Community Land model (CLM). Natl. Cent. For. Atmosph. Res., Boulder Co.Technical NoteTN 461.

Oncley, S.P., Foken, T., Vogt, R., Kohsiek, W., 2007. The energy balance experiment EBEX-2000. Part I: overview and energy balance. Boundary Layer Meteorol. 123 (1), 1–28.

Ortega-Farias, S., Poblete-Echeverría, C., Brisson, N., 2010. Parameterization of a two-layer model for estimating vineyard evapotranspiration using meteorological measurements. Agric. For. Meteorol. 150 (2), 276–286.

Paço, T.A., Ferreira, M.I., Rosa, R.D., Paredes, P., Rodrigues, G.C., 2012. The dual crop coefficient approach using a density factor to simulate the evapotranspiration of a peach orchard: SIMDualKc model versus eddy covariance measurements. Irrig. Sci. 30 (2), 115–126.

Picón-Toro, J., González-Dugo, V., Uriarte, D., Mancha Ramirez, L.A., Testi, L., 2012. Effects of canopy size and water stress over the crop coefficient of a "tempranillo" vineyard in south-western Spain. Irrig. Sci. 30 (5), 419–432.

Poblete-Echeverría, C.A., Ortega-Farias, S.O., 2013. Evaluation of single and dual crop coefficients over a drip-irrigated Merlot vineyard (*Vitis vinifera* L.) using combined measurements of sap flow sensors and an eddy covariance system. Aust. J. Grape Wine Res. 19 (2), 249–260.

Prueger, J.H., Hipps, L.E., Cooper, D.I., 1996. Evaporation and the development of the local boundary layer over an irrigated surface in an arid region. Agric. For. Meteorol. 78 (3-4), 223–237.

Rosenberg, N.J., Blad, B.L., Verma, S.B., 1983. Microclimate: the Biological Environment. Wiley, New York.

Sakuratani, T., 1981. A heat balance method for measuring water flux in the stem of intact plants. J. Agric. Meteorol. 37 (1), 9–17.

Sánchez, J.M., López-Urrea, R., Rubio, E., González-Piqueras, J., Caselles, V., 2014. Assessing crop coefficients of sunflower and canola using two-source energy balance and thermal radiometry. Agric. Water Manage. 137 (137), 23–29.

Schlesinger, W.H., Jasechko, S., 2014. Transpiration in the global water cycle. Agric. For. Meteorol. 189–190 (6), 115–117.

Smith, D.M., Jarvis, P.G., Odongo, J.C.W., 1997. Energy budgets of windbreak canopies in the Sahel. Agric. For. Meteorol. 86 (96), 33–49.

Soegaard, H., Boegh, E., 1995. Estimation of evapotranspiration from a millet crop in the Sahel combining sap flow, leaf area index and eddy correlation technique. J. Hydrol. 166 (3–4), 265–282.

Sun, H., Shao, L., Liu, X., Miao, W., Chen, S., Zhang, X., 2012. Determination of water consumption and the water-saving potential of three mulching methods in a jujube orchard. Eur. J. Agron. 43 (43), 87–95.

Sutanto, S.J., Van den Hurk, B., Dirmeyer, P.A., Seneviratne, S.I., Röckmann, T., Trenberth, K.E., et al., 2014. HESS opinions "A perspective on isotope versus non-isotope approaches to determine the contribution of transpiration to total evaporation. Hydrol. Earth Syst. Sci. 18 (8), 2815–2827.

Trambouze, W., Voltz, M., 2001. Measurement and modelling of the transpiration of a Mediterranean vineyard. Agric. For. Meteorol. 107 (2), 153–166.

Wang, J., Mitsuta, Y., 1992. Evaporation from the desert: some preliminary results of HEIFE. Boundary Layer Meteorol. 59 (4), 413–418.

Wang, L.X., Caylor, K.K., Villegas, J.C., Barron-Gafford, G.A., Breshears, D.D., Huxman, T.E., 2010. Partitioning evapotranspiration across gradients of woody plant cover: assessment of a stable isotope technique. Geophys. Res. Lett. 37 (9), 232–256.

Williams, L.E., Ayars, J.E., 2005. Grapevine water use and the crop coefficient are linear functions of the shaded area measured beneath the canopy. Agric. For. Meteorol. 132 (3–4), 201–211.

Williams, L.E., Phene, C.J., Grimes, D.W., Trout, T.J., 2003a. Water use of mature Thompson seedless grapevines in California. Irrig. Sci. 22 (1), 11–18.

Williams, L.E., Phene, C.J., Grimes, D.W., Trout, T.J., 2003b. Water use of young Thompson seedless grapevines in California. Irrig. Sci. 22 (1), 1–9.

Williams, D.G., Cable, W., Hultine, K., Hoedjes, J.C.B., Yepez, E.A., Simonneaux, V., et al., 2004. Evapotranspiration components determined by stable isotope, sap flow and eddy covariance techniques. Agric. For. Meteorol. 125 (3–4), 241–258.

Yan, B., Zhu, G., Su, Y., Zhang, K., Han, T., Ma, J., et al., 2015. Hysteresis loops between canopy conductance of grapevines and meteorological variables in an oasis ecosystem. Agric. For. Meteorol. 214–215, 319–327.

Yang, P., Hu, H., Tian, F., Zhang, Z., Dai, C., 2016. Crop coefficient for cotton under plastic mulch and drip irrigation based on eddy covariance observation in an arid area of northwestern China. Agric. Water Manage. 171, 21–30.

Zhang, Y., Kang, S., Ward, E.J., Ding, R., Zhang, X., Zheng, R., 2011. Evapotranspiration components determined by sap flow and micro-lysimetry techniques of a vineyard in northwest China: dynamics and influential factors. Agric. Water Manage. 98 (8), 1207–1214.

Zhao, P., Li, S., Li, F., Du, T., Tong, L., Kang, S., 2015. Comparison of dual crop coefficient method and Shuttleworth Wallace model in evapotranspiration partitioning in a vineyard of northwest China. Agric. Water Manage. 160, 41–56.

Zhao, L., Zhao, W., 2015. Canopy transpiration obtained from leaf transpiration, sap flow and fao-56 dual crop coefficient method. Hydrol. Process. 29 (13), 2983–2993.

Zhu, G.F., Li, Z.Z., Su, Y.H., Ma, J.Z., Zhang, Y.Y., 2007. Hydrogeochemical and isotope evidence of groundwater evolution and recharge in Minqin Basin, northwest China. J. Hydrol. 333 (2), 239–251.

Zhu, G.F., Su, Y.H., Feng, Q., 2008. The hydrochemical characteristics and evolution of groundwater and surface water in the Heihe River Basin, northwest China. Hydrogeol. J. 16 (1), 167–182.

Zhu, G.F., Li, X., Su, Y.H., Zhang, K., Bai, Y., Ma, J.Z., et al., 2014. Simultaneously assimilating multivariate data sets into the two-source evapotranspiration model by Bayesian approach: application to spring maize in an arid region of northwestern China. Geosci. Model Dev. 7 (4), 1467–1482.

Zhu, G.F., Zhang, K., Li, X., Liu, S.M., Ding, Z.Y., Ma, J.Z., et al., 2016a. Evaluating the complementary relationship for estimating evapotranspiration using the multi-site data across north China. Agric. For. Meteorol. 230-231, 33–34.

Zhu, G., Li, X., Zhang, K., Ding, Z., Han, T., Ma, J., et al., 2016b. Multi-model ensemble prediction of terrestrial evapotranspiration across north china using bayesian model averaging. Hydrol. Processes 30 (16), 2861–2879.